

A micron-sized GMR sensor with a CoCrPt hard bias

Zheng Yang(郑洋)¹, Qu Bingjun(曲炳郡)^{1,†}, Liu Xi(刘晰)³, Wei Dan(韦丹)², Wei Fulin(魏福林)³, Ren Tianling(任天令)¹, and Liu Litian(刘理天)¹

(1 Institute of Microelectronics, Tsinghua University, Beijing 100084, China)

(2 Laboratory of Advanced Materials, Department of Materials Science and Engineering, Tsinghua University, Beijing 100084, China)

(3 Key Laboratory of Magnetism and Magnetic Materials, Research Institute of Magnetic Materials, Lanzhou University, Gansu 730000, China)

Abstract: A GMR (giant magneto-resistive) spin valve sensor for magnetic recording has been designed in an attempt to solve the Barkhausen noise problem in small-sized GMR sensors. In this study, the GMR ratio of the top-pinned spin valve is optimized to a value of 13.2%. The free layer is magnetized perpendicular to the pinned layer by a CoCrPt permanent magnetic bias so that a linear magnetic field response can be obtained. An obvious improvement on performance is observed when the permanent magnetic bias is magnetized, while the GMR sensor has a steadier MR–*H* loop and a smaller coercive field.

Key words: GMR; spin-valve; magnetic stabilization; Barkhausen noise

DOI: 10.1088/1674-4926/31/2/024005

PACC: 7570P

1. Introduction

GMR (giant magneto-resistive) multilayers have been widely utilized because of their excellent characteristics since they were discovered in 1988^[1]. The magnetic sensor is the most common application of GMR. As the recording density in magnetic media increases, the size and aspect ratio of read sensors must be reduced accordingly. As a result, the GMR sensor will suffer from Barkhausen noise which originates from domain activities^[2]. Because the basic GMR characteristic is nonlinear, some steps must be taken to obtain a certain level of linearity in signal response. This leads to the development of tail stabilization, in which the free layer of the GMR sensor is stabilized in a single domain state by a pair of permanent magnets (PM) or anti-ferromagnetic (AF) exchange^[3–5].

In the AM domain bias scheme, a pair of AF exchange tabs which provides bias field overlaps with the two ends of the free layer. However, the challenge is that two magnetic annealing process steps are needed to achieve the orthogonal magnetization orientation of the pinned layer and the free layer. That is to say, two AF materials with distinctively different blocking temperatures are required in order to minimize the cross interference between the two magnetic annealing steps^[6].

In the PM domain bias scheme, a pair of hard magnets abutting against the ends of the sensor provides the magnetic field which magnetizes the free layer of the spin valve to a single domain state^[4]. However, in order to ensure sufficient sensor stability, the moment density of the PM has to be sufficiently high. So, the magnetic flux from the PM stiffens the magnetization rotation of the ring regions of the free layer, and that limits the sensor's activity^[7].

We choose the PM domain bias scheme for the magnetic sensor because it is simpler in process than the AM domain bias scheme. Nevertheless, there are other problems in the pro-

cess, such as the alignment of the PM and the sensor, and temperature control. The process of the sensor is introduced. The MR loops of the sensor before and after the PM bias is magnetized are compared, and the existence of the hard bias largely reduces the Barkhausen noise.

2. Experiments

A simple spin-valve structure of Ta/NiFeCr/CoFe/Cu/CoFe/MnIr/Ta is chosen to fabricate the read head, as shown in Fig. 1. The layers are: seed layer (Ta/NiFeCr), free layer (CoFe), spacer (Cu), pinned layer (CoFe), antiferromagnetic layer (MnIr) and capping layer (Ta), respectively. The free layer and pinned layer are separated by the Cu spacer layer. The magnetic moment of the CoFe pinned layer is generally fixed along the transverse direction by exchange coupling with the MnIr antiferromagnetic layer. The CoFe free layer is magnetized longitudinally by the permanent magnetic bias and is also allowed to rotate in response to signal fields. When the magnetic moment of the free layer rotates parallel/anti-parallel to the magnetic moment of the pinned layer, the resistance of spin-valve becomes smaller/larger.

This spin-valve structure has the following advantages:

(1) The spin-valve is top-pinned, so that a magnetic anneal-

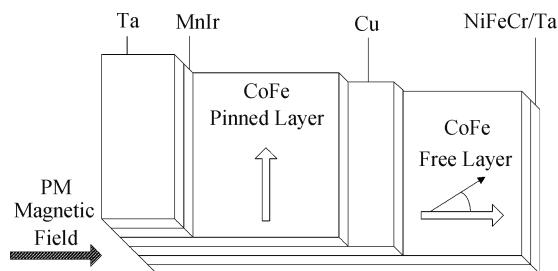


Fig. 1. Schematic of the GMR spin valve.

[†] Corresponding author. Email: qubj@mail.tsinghua.edu.cn

Received 3 July 2009, revised manuscript received 15 September 2009

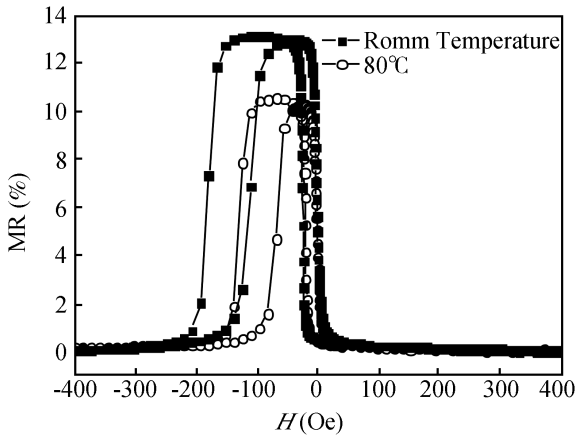


Fig. 2. MR–*H* loops of the GMR multilayer at room temperature and 80 °C.

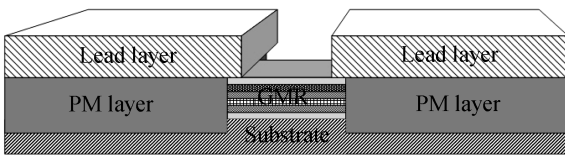


Fig. 3. Structure of the sensor.

ing process is unnecessary.

(2) The CoFe free layer has a large spin-relative scattering coefficient, so a large GMR ratio can be obtained^[8].

(3) NiFeCr, which increases the grain size of crystalline films, is highly beneficial to maximize the MR ratio by reducing parasitic grain boundary scattering^[9].

The spin-valve films are deposited by a conventional magnetron sputtering system with six targets from the Lesker Company. The base pressure is lower than 1×10^{-7} Torr, and the deposit pressure is 0.198 Pa. The MR ratio of GMR multilayers was measured by four-point probe resistivity measurement. The thickness of each layer was optimized and the structure of the GMR multilayers was finally identified as Ta(3.3 nm)/NiFeCr(2.9 nm)/CoFe(3.2 nm)/Cu(1.8 nm)/CoFe(3.2 nm)/MnIr(11 nm)/Ta(1.9 nm). An MR ratio of 13.2% was obtained.

Because the GMR is composed of different materials, these materials may interpenetrate as the temperature rises. This will cause degradation of the GMR performance. However, a temperature decrease does not quite affect the MR ratio. We measured the GMR multilayer performance at 80 °C, which was defined as the highest temperature for military electronic products. The GMR performance at room temperature was also measured as a contrast. Figure 2 shows the MR–*H* loop of the spin-valve at room temperature and 80 °C. The exchange field H_{ex} and MR ratio both decrease when the temperature reaches 80 °C: H_{ex} drops from 145 Oe to 98 Oe and the MR ratio drops from 13.2% to 10.6%. But the area used for magnetic detection in low field is not affected, and the coercivity H_c is maintained at 9.5 Oe. This characteristic shows that this GMR multilayer can be used at high temperatures.

As shown in Fig. 3, the PM layer abutting against the ends of the sense region provides a hard bias stabilization field to

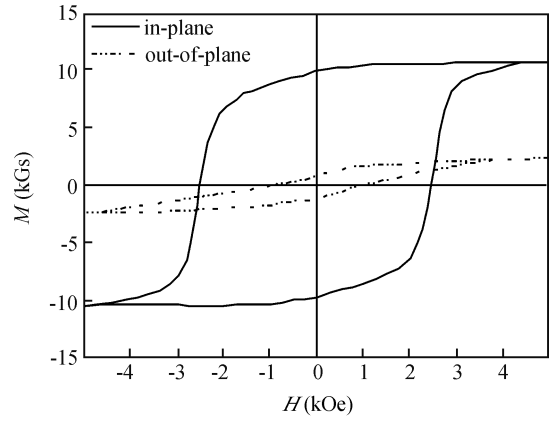


Fig. 4. *M*–*H* hysteresis loop of the CoCrPt PM layer.

the free layer. Misalignment of the PM layer edge to the sense region can reduce the coupling effect of the field on the free layer, and misalignment of the lead layer, which conducts current to the films of the sense region, to the sense region can cause large contact resistance which might reduce the MR ratio of the whole sensor. Thus a new fabrication process that creates a contiguous junction between the sense region and the PM/lead layer is used.

The GMR multilayer was deposited and then patterned with an aspect ratio of $2 \mu\text{m} : 1 \mu\text{m}$ by optical lithography and an IBE (ion beam etching) process. In the process of sputtering the PM layer, a multilayer SiO₂ (substrate)/MgO (seed layer)/CrW (underlayer)/CoCr (intermediate layer) was first deposited, so that the CoCrPt hard bias layer could be deposited without a high-temperature process which may destroy the GMR multilayer structure^[10]. The thickness of the GMR layer is about 30 nm, but the multilayer layer underneath the CoCrPt PM layer is 53 nm thick. So a wet etching process with BHF (HF and NH₄F mixed solution) was used to etching the SiO₂ substrate with an accurate depth of 70 nm. This process ensures that the PM layer was aligned to the free layer of GMR. Then the PM layer and the lead layer were deposited by optical lithography and a sputtering process. Finally, the passivation layer was deposited.

3. Results and discussion

As discussed above, the moment density of the CoCrPt PM layer has to be sufficiently high in order to provide a magnetic field to stabilize the free layer in a single domain state. The hysteresis loop of the CoCrPt layer is shown in Fig. 4. The residual magnetization of the CoCrPt layer is about 10 kGs in-plane, and very small out-of-plane. This character ensures a sufficiently large magnetic bias field for stabilization and avoids the influence of the data storage medium.

Typically, the resistance of the GMR sensor reaches minimum/maximum when the pinned and the free layer are parallel/anti-parallel. We define the angle between the two layers as θ , the resistance in the two situations as R_{min} and R_{max} , and $\Delta R = R_{max} - R_{min}$. Then, the GMR response can be given by $R = R_{min} + (\Delta R/2) \sin \theta$. As shown in Fig. 1, the pinned layer magnetization was oriented transversely by exchange coupling, and the free layer magnetization was oriented

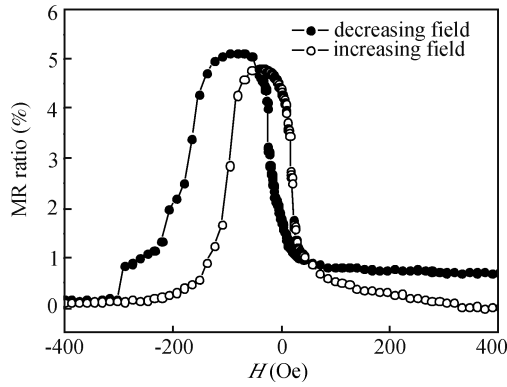


Fig. 5. MR–H loop before the PM bias is magnetized.

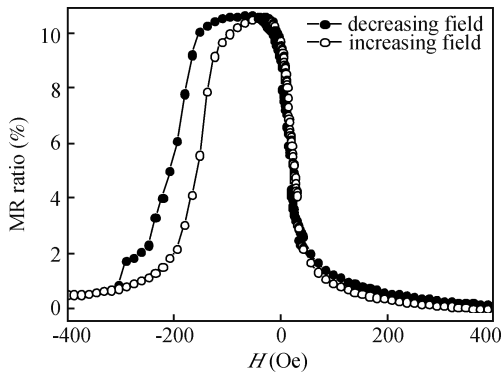


Fig. 6. MR–H loop after the PM bias is magnetized.

longitudinally, θ equaled 90° . When reading data from storage media, angular deviations of the free layer magnetization due to the media magnetic field result in a quasi-linear output^[11]. The linear response of the sensor is very important in reading data and is achieved by careful consideration of magnetization directions.

Accidental current bursts lasting only a few nanoseconds can cause the sensor films to reach very high temperatures and lead to direct sensor breakdown. So electrostatic discharge and high current should be avoided while testing the sensor. ESD protection is used and the soldering process in the electrical connection is substituted by a bonding process. The total resistance of the sensor is about 63–69 Ω and the MR ratio is 10.6%. The MR ratio is smaller than the spin-valve films, which is because the magnetic domains on the margin of a mesoscopic ferromagnetic device are pinned by an edge demagnetizing field and thus have no MR effect. Furthermore, the lead and the contact regions have lead resistance and contact resistance. These additional resistances also reduce the MR ratio of the sensor.

The MR–H loops of the sensor before and after the CoCrPt PM layer is magnetized are shown in Figs. 5 and 6 respectively, where the signal field is imposed transversely. The coercivity of the sensor with a magnetized PM layer (shown in Fig. 6) is much smaller than the GMR multilayer as shown in Fig. 2, which is good for the performance of magnetic field detection. This is because the size of the GMR film of the sensor is much smaller and the shape demagnetization factor is different in a 2 : 1 micron-sized device. As seen in Fig. 5, before the PM layer is magnetized, the Barkhausen noise caused by the do-

main hopping is obvious and the MR–H loop is very unstable. After the PM layer is magnetized (shown in Fig. 6), the situation is significantly improved and the MR ratio also increases from 5.3% to 10.6%.

The linear region of the sensor is from –25 Oe to 50 Oe. This linear region is relatively narrow because the size of the patterned GMR film (1–2 μm) is much larger than the exchange bias length l_{ex} of the NiFeCr/CoFe free layer (usually 100 nm). If the height of the GMR sensor is comparable with l_{ex} , the magnetic moment will rotate consistently, the effect of the hard magnetic bias will be much better, and the linear region will be largely increased.

There are at least three forces at work to induce transverse magnetization of the free layer, which makes the linear region deviate from the zero magnetic field point. First, magnetostatic coupling between the free and pinned layer usually has a substantial effect. This coupling favors antiparallel alignment of the two layers, and its magnitude depends on the thickness and height of the sensor. Secondly, ferromagnetic interlayer coupling between the free and pinned layer, which favors parallel alignment, is also present; its magnitude depends on variables such as substrate flatness and film morphologies, which are difficult to control. Thirdly, the applied sense current in the sensor also creates a significant transverse magnetic field, which mainly depends on the current polarity and magnitude^[12]. For our design, the magnetostatic coupling is larger than the sum of the ferromagnetic coupling and the current bias field. So, the linear region deviates from the zero magnetic field point.

4. Conclusion

A micron-sized sensor based on GMR spin-valve film is fabricated. The PM domain bias scheme is chosen to solve the Barkhausen noise problem, because it is simpler in process than the AM domain bias scheme. The alignment of the PM and the sensor, and the temperature control, are solved by a special fabrication process. Transverse magnetization of the pinned layer and longitudinal magnetization of the free layer are achieved by exchange coupling and a hard magnetic bias. This makes the sensor have a linear response under low magnetic field, where the MR ratio of the sensor is 10.6% and the linear region is from –25 Oe to 50 Oe. Obvious improvements, such as a larger MR ratio, smaller coercivity and steady response, are achieved with a magnetized PM bias layer for a small geometry sensor. The linear region of the sensor needs to be improved by reducing the size of the GMR film to be comparable to the exchange bias length l_{ex} and carefully optimizing the effects that are at work to induce transverse orientation of the free layer.

References

- [1] Baibich M N, Broto J M, Fert A, et al. Giant magnetoresistance of (001)Fe/(001)Cr magnetic superlattice. *Phys Rev Lett*, 1988, 61: 2472
- [2] Wallash A. A study of voltage function, noise and magnetic instability in spin valve GMR recording heads. *IEEE Trans Magn*, 1998, 34(4): 1450
- [3] Tsang C H, Fontana R E Jr, Lin T, et al. Design, fabrication, and performance of spin-valve read heads for magnetic recording applications. *IBM J Res Dev*, 1998, 42: 103

- [4] Lambertson R, Seigler M, Pelhos K, et al. Current-in-plane GMR trilayer head design for hard-disk drives: characterization and extendibility. *IEEE Trans Magn*, 2007, 43: 645
- [5] Fernandez-Outon L E, Vallejo-Fernandez G, Manzoor S, et al. Thermal instabilities in exchange biased materials. *Journal of Magnetism and Magnetic Materials*, 2006, 303: 296
- [6] Dobrynin A N, Prozorov R. Characteristic temperatures of exchange biased systems. *J Appl Phys*, 2007, 102: 043902
- [7] Zhu J G, Zheng Y, Liao S. Patterned exchange stabilized spin valve heads at very narrow track width. *IEEE Trans Magn*, 2001, 37: 1723
- [8] Parkin S S. Dramatic enhancement of interlayer exchange coupling and giant magnetoresistance in $\text{Ni}_{81}\text{Fe}_{19}/\text{Cu}$ multilayers by addition of thin Co interface layers. *Appl Phys Lett*, 1992, 61: 1358
- [9] Lee C L, Devasahayam A J, Hu C C, et al. Critical thickness effects of NiFeCr-CoFe seed layers for spin. *IEEE Trans Magn*, 2004, 40: 2209
- [10] Liu X, Li Z H, Li S T, et al. Preparation of longitudinally oriented CoCrPt thin film in GMR head at room temperature. *IEEE Trans Magn*, 2008, 44: 2858
- [11] Lu Z Q, Pan G. New domain biasing techniques for nanoscale magneto-electronic devices. *Springer Series in Materials Science*, 2007, 94: 187
- [12] Tsang C H, Fontana R E, Lin T, et al. Design, fabrication, and performance of spin-valve read heads for magnetic recording applications. *IBM Journal of Research and Development*, 1998, 42: 103